DRUG PARTICLES SMALLER THAN EVER BEFORE

Working with you to enhance drug effectiveness and targeting

Our global experts in nanotechnology and drug particle engineering can help your drugs reach their full therapeutic potential. With the unique ability to produce nanoparticles as small as 10 nm, our award-winning Controlled Expansion of Supercritical Solutions (CESS®) technology can increase dissolution rates and improve bioavailability. Together, we can initiate a new era of novel drug development and enable more patients around the world to benefit from next-generation drug therapies.

nanoform
small is powerful

Contact Nanoform to unlock the potential of your molecules +358 29 370 0150

nanoform.com | info@nanoform.com

@NanoformF Nanoform

DRUG DEVELOPMENT RESEARCH 77 : 285–299 (2016)

Research Article

Synthesis and Pharmacological Evaluation of Indole Derivatives as Deaza Analogues of Potent Human Neutrophil Elastase Inhibitors

Letizia Crocetti,[1] Igor A. Schepetkin,[2] Giovanna Ciciani,[1] Maria Paola Giovannoni,[1]* Gabriella Guerrini,[1] Antonella Iacovone,[1] Andrei I. Khlebnikov,[3] Liliya N. Kirpotina,[2] Mark T. Quinn,[2] and Claudia Vergelli[1]

[1]*NEUROFARBA, Sezione di Farmaceutica e Nutraceutica, Università degli Studi di Firenze, Via Ugo Schiff 6, 50019 Sesto Fiorentino, Italy*

[2]*Department of Microbiology and Immunology, Montana State University, Bozeman, MT 59717*

[3]*Department of Biotechnology and Organic Chemistry, Tomsk Polytechnic University, Tomsk 634050, Russia and Department of Chemistry, Altai State Technical University, Barnaul, Russia*

Strategy, Management and Health Policy				
Enabling Technology, Genomics, Proteomics	Preclinical Research	Preclinical Development Toxicology, Formulation Drug Delivery, Pharmacokinetics	Clinical Development Phases I-III Regulatory, Quality, Manufacturing	Postmarketing Phase IV

ABSTRACT A number of N-benzoylindoles were designed and synthesized as deaza analogs of previously reported potent and selective HNE inhibitors with an indazole scaffold. The new compounds containing substituents and functions that were most active in the previous series were active in the micromolar range (the most potent had $IC_{50} = 3.8$ μM) or inactive. These results demonstrated the importance of N-2 in the indazole nucleus. Docking studies performed on several compounds containing the same substituents but with an indole or an indazole scaffold, respectively, highlight interesting aspects concerning the molecule orientation and H-bonding interactions, which could help to explain the lower activity of this new series. Drug Dev Res 77 : 285–299, 2016. © 2016 Wiley Periodicals, Inc.

Key words: indoles; human neutrophil elastase (HNE); inhibitors

INTRODUCTION

Neutrophil serine proteases (NSPs) are granule-associated enzymes mainly known for their role in the intracellular killing of pathogens and are stored into acidic granules tightly bound with proteoglycans [Reeves et al., 2002]. Their extracellular release following neutrophil activation is traditionally considered the main cause for tissue damage at sites of inflammation [Pham, 2006]. This protease family consists of neutrophil elastase (NE), proteinase 3, cathepsin G and the recently discovered NSP4 [Perera et al., 2012].

Human neutrophil elastase (HNE) is a small, soluble protein of aprroximately 30 kDa with 218 amino acid residues that are stabilized by four disulfide bridges [Sihna et al., 1987]. HNE is a basic glycoprotein with a catalytic triad, consisting of Ser195, His57, and Asp102 [Bode et al., 1989]. HNE is currently considered a

[†]This research was supported in part by National Institutes of Health IDeA Program COBRE Grant GM110732; a USDA National Institute of Food and Agriculture Hatch project; Montana University System Research Initiative: 51040-MUSRI2015-03; and the Montana State University Agricultural Experiment Station.

*Correspondence to: Maria Paola Giovannoni, Dipartimento di NEUROFARBA, Via Ugo Schiff 6, Sesto Fiorentino 50019 Firenze. E-mail: Mariapaola.Giovannoni@unifi.it

Received 28 June 2016; Accepted 16 July 2016

Published online in Wiley Online Library (wileyonlinelibrary.com). DOI: 10.1002/ddr.21323

multifunctional enzyme involved in the killing of pathogens and in the regulation of inflammation and tissue homeostasis [Pham, 2006] via its proteolytic actions against a variety of extracellular matrix proteins, such as elastin, collagen, fibronectin, laminin, proteoglycans [Chua and Laurent, 2006], and some matrix metalloproteinases [Geraghty et al., 2007]. HNE appears to play an important role in chemotaxis and migration of neutrophils to inflammatory mediators by the splitting of adhesion molecules at cell junctions [Cepinskas et al., 1999; Hermant et al., 2003]. The serpin family of endogenous inhibitors, including α-$_1$ antitripsin (α_1-AT), α_2-macroglobuline, elafin, and secretory leucocyte protease inhibitor (SLPI), is able to reduce the tissue damage of HNE under physiological conditions to regulate inflammatory processes [Potempa et al., 1994; Tremblay et al., 2003; Heutinck et al., 2010]. Alteration of the balance between HNE and serpin activity can contribute to certain pathologies, especially in the lung, where an excess of HNE activity leads to hydrolysis of elastin and other extracellular matrix proteins, such as inflammatory mediators, cell surface receptors, and lung surfactants. Moreover, HNE can cause the activation of other proteases and cytokines, resulting in a massive amplification of the inflammatory response [Heutinck et al., 2010; Korkmaz et al., 2008; Korkmaz et al., 2010]. The main pulmonary diseases involving HNE are chronic obstructive pulmonary disease (COPD) [O'Donnell et al., 2004; Hogg et al., 2004], acute respiratory distress syndrome (ARDS) [Wang et al., 2009], and acute lung injury [Kawabata et al., 2002].

Cystic fibrosis (CF) is a life threatening genetically based disease where excessive mucus production is associated with a massive influx of neutrophils and HNE release [Voynow et al., 2008; Gifford and Chalmers, 2014]. HNE is also involved in other inflammatory disorders, including psoriasis [Meyer-Hoffert et al., 2004], dermatitis, atherosclerosis [Henrisken and Sallenave, 2008], rheumatoid arthritis [Hilbert et al., 2002], and various types of cancer [Sato et al., 2006; Moroy et al., 2012]. Lastly, HNE plays a central role both in acute pathogenesis and chronic functional restoration after brain traumatic injury [Semple et al., 2015].

In light of the evidence summarized above, HNE represents an important therapeutic target [Groutas et al., 2011; Henriksen, 2014]. The classification of HNE inhibitors is based on their structure (peptide and non-peptide) or on their mechanism of action (mechanism-based inhibitors [Zhong and Groutas, 2004], acylating-enzyme inhibitors [Lucas et al., 2011], transition-state analogs, and noncovalent inhibitors [Sjö, 2012]). At present, only two drugs are available for clinical use: Prolastin® (purified α_1-AT) for the treatment of α_1-antitripsin deficiency [Bayer Corp, 2002] and Sivelestat (Elaspol® 100, Figure 1) marketed in Japan and Korea for the treatment of acute lung injury associated with systemic inflammatory response syndrome [Iwata et al., 2010]. Two HNE inhibitors are currently in clinical trials: AZD9668 (Alvelestat) for bronchiectasis and COPD [Vogelmeier et al., 2012; Stockley et al., 2013] and BAY 85-8501, a novel dihydropyrimidinone for the treatment of pulmonary disease (Figure 1) [Von Nussbaum et al., 2015].

We recently discovered novel HNE inhibitors belonging to different chemical classes [Crocetti et al., 2011; Crocetti et al., 2013; Giovannoni et al., 2015]. These compounds are competitive, pseudo-irreversible HNE inhibitors and show appreciable selectivity toward HNE versus the other kinases. The most interesting HNE inhibitors had an *N*-benzoylindazole scaffold (structure **A**, Figure 2) and had activity in the nanomolar range (IC_{50} = 7-80 nM). The essential requirement for activity was the carbonyl group at position *1*, which is the point of attack of Ser195 in the active site [Crocetti et al., 2013].

In the present paper, we report the synthesis of a new series of indole derivatives (**B**) as deaza analogs of the previously described potent indazoles in order to evaluate the importance of the nitrogen at position *2* for HNE inhibitory activity (Figure 2). In the indole scaffold, we inserted the substituents and functions which in the previous series afforded the best results, as well as additional modifications. The results of these studies provide new information on the importance of various substructures in the development of new synthetic HNE inhibitors.

METHODS AND MATERIALS

Chemistry

All new compounds were synthesized as reported in Figures 3–5, and the structures confirmed on the basis of analytical and spectral data. Figure 3 shows the synthetic pathway used to obtain the final compounds bearing an ester function (**2a-g** and **3a,b**), a cyano group (**4a,b**) [Wang and Chuang, 1997], or a phenylamide (**5a-g**) at position 3, respectively. The starting compounds **1a-d** were synthesized as previously reported [Shahidul et al., 2006; Spinks et al., 2003; Yuen et al., 2013; Veale et al., 2015]. The introduction at N-1 of the benzoyl meta or para substitution was performed by treatment with the suitable benzoyl chloride either with sodium hydride in anhydrous tetrahydrofuran (THF) at room temperature (compounds **2c-g, 3a,b, 4a,b)** or with a catalytic amount

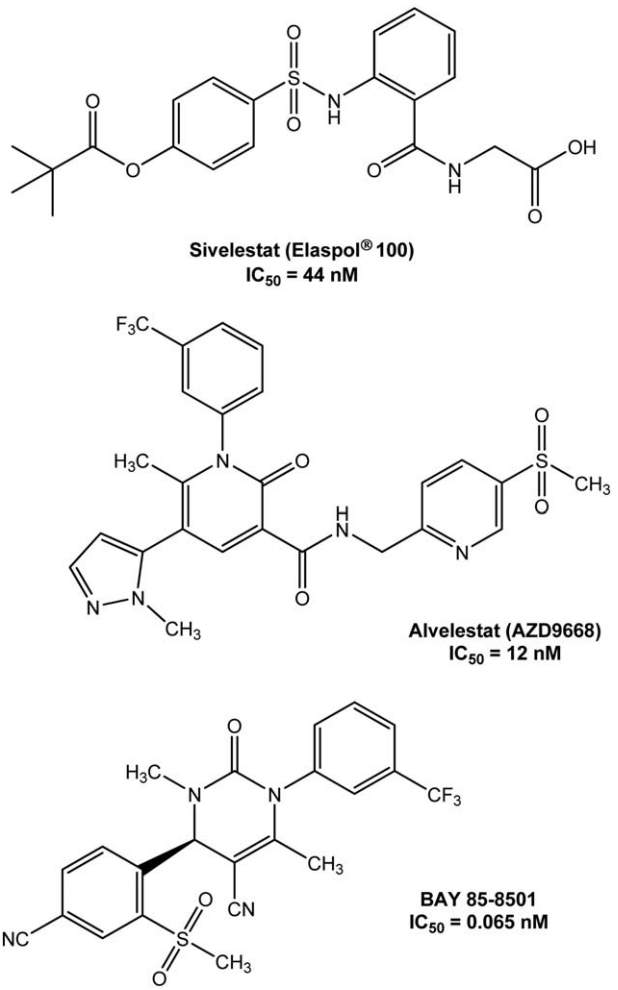

Fig. 1. HNE inhibitors.

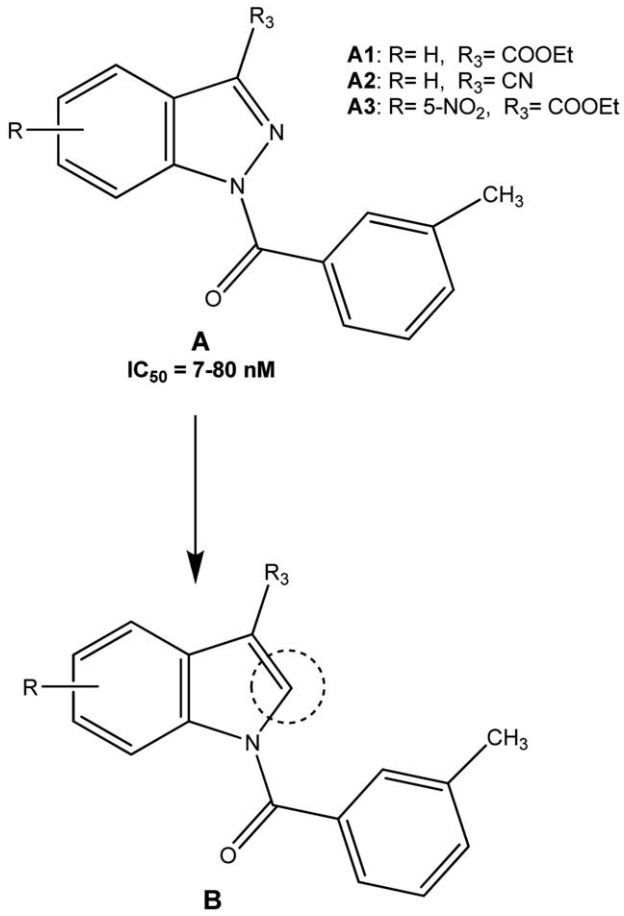

Fig. 2. Indazole derivatives (**A**) and indole derivatives (**B**) as deaza analogs.

of triethylamine in dichloromethane (compounds **5a-e**). The latter method, using the appropriate sulfonylchloride, was used for the sulfonamide derivatives **5f,g**. Compounds **2a** and **2b**, lacking the amide function at position *1*, were synthesized by a cross-coupling reaction (**2a**) with 3-methylphenylboronic acid, using copper acetate as catalyst, and triethylamine in dichloromethane or with 3-methylbenzyl chloride in anhydrous acetonitrile and K_2CO_3 (**2b**).

We next inserted a bromine or a nitro at positions 5 and 6 of indole nucleus (Figure 4). Starting from precursors **6a-c**, synthesized as described previously [Tantak et al., 2013; Li et al., 2012; DeGraw and Goodman, 1964], we obtained the final compounds **7a-e** using the same procedure as described in Figure 3. The 5-NO_2 derivative **7e** was then converted by catalytic reduction with a Parr instrument into the corresponding 5-amino compound **8**, which, in turn, was treated with acetyl chloride in dichloromethane and triethylamine, resulting in the final compound **9**.

Starting from compounds **10a,b** [Panatur et al., 2013; Sudhakara et al., 2009] and following the same procedures reported in Figures 3 and 4, we obtained the desired **11a-d** as isomers of **2c,d** (5-unsubstituted) and **7d,e** (5-NO_2).

Experimental

All melting points were determined using a Büchi apparatus (New Castle, DE) and are uncorrected. Extracts were dried over Na_2SO_4, and the solvents were removed under reduced pressure. Merck F-254 commercial plates (Merck, Durham, NC) were used for analytical TLC to follow the course of reactions. Silica gel 60 (Merck 70–230 mesh, Merck, Durham, NC) was used for column chromatography. ^{1}H NMR and ^{13}C NMR spectra were recorded on an Avance 400 instrument (Bruker Biospin Version 002 with SGU, Bruker Inc., Billerica, MA). Chemical shifts (δ) are reported in ppm to the nearest 0.01 ppm using the solvent as an internal standard. Coupling constants (J values) reported in Hz were calculated using

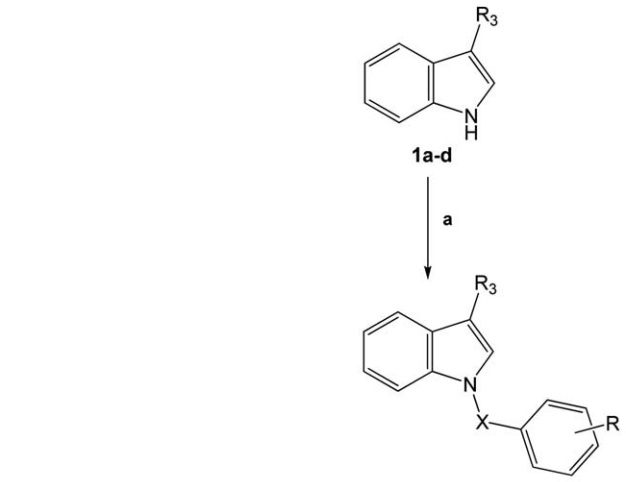

1	R_3
a	COOEt
b	CH_2COOEt
c	CN
d	CONHPh

2	X	R
a	-	m-CH_3
b	CH_2	m-CH_3
c	CO	m-CH_3
d	CO	p-CH_3
e	CO	p-Cl
f	CO	m-Cl
g	CO	p-F

3, 4	X	R
a	CO	m-CH_3
b	CO	p-CH_3

5	X	R
a	CO	p-Cl
b	CO	m-Cl
c	CO	p-CH_3
d	CO	p-F
e	CO	m-F
f	SO_2	p-CH_3
g	SO_2	p-Cl

Fig. 3. Synthesis of the final compounds **2a-g, 3a,b, 4a,b,** and **5a-g.** Reagents and conditions: a) for **2a**: 3-methylphenyl boronic acid, $(CH_3COO)_2Cu$, El_3N, anhydrous CH_2Cl_2, r.t., 24 h; for **2b**: 3-methylhenzy1chloride. K_2CO_3. anhydrous CH_3CN. 90°C, 3 h; for **2e-9, 3a,b** and **4a,b**: NaH. A-COCI. anhydrous THF. r.t., 24 h; for **5a-e**: Ar-COCL, Et_3N. anhydrous CH_2Cl_2, 0°C. 2h; r.t., 1-8 h: for **5f,g**: Ar-SO_2CI, Et_3N. anhydrous CH_2Cl_2, 0°C. **2h**: r.t., 3-6 h.

TopSpin 1.3 software (Nicolet Instrument Corp., Madison, WI) and are rounded to the nearest 0.1 Hz. Mass spectra (m/z) were recorded on an ESI-TOF mass spectrometer (Brucker Micro TOF, Bruker Inc., Billerica, MA), and reported mass values are within the error limits of ± 5 ppm mass units. Microanalyses indicated by the symbols of the elements or functions were performed with a Perkin–Elmer 260 elemental analyzer (PerkinElmer, Inc., Waltham, MA) for C, H, and N, and the results are within ±0.4% of the theoretical values, unless otherwise stated. Reagents and starting material were commercially available.

Ethyl 1-(m-tolyl)-1H-indole-3-carboxylate (2a)

A mixture of dry CH_2Cl_2 (8 mL), **1a** (0.53 mmol), 3-methylphenylboronic acid (1.06 mmol), $Cu(Ac)_2$ (0.79 mmol), and Et_3N (1.06 mmol) was stirred at room temperature for 24 h. The solution was first washed with water (3 x 20 mL), and then with 33% aqueous ammonia (3 x 5 mL). The organic phase was dried over sodium sulfate, and the solvent was evaporated in vacuo to obtain the final compound **2a**, which was purified by column chromatography using cyclohexane/ethyl acetate (5:1) as eluent. Yield = 19%; oil. ^{1}H NMR ($CDCl_3$) δ 1.46 (t, 3H, OCH_2CH_3, J = 7.2 Hz), 2.48 (s, 3H, CH_3), 4.44 (q, 2H, OCH_2CH_3, J = 7.2 Hz), 7.26-7.36 (m, 5H, Ar), 7.45 (t, 1H, Ar, J = 8.2 Hz), 7.53 (d, 1H, Ar, J = 8.0 Hz), 8.04 (d, 1H, Ar, J = 2.4 Hz), 8.28 (d, 1H, Ar, J = 8.4 Hz). ^{13}C NMR ($CDCl_3$) δ 14.60 (CH_3), 21.42 (CH_3), 59.85 (CH_2), 67.00 (C), 105.00 (C), 111.08 (CH), 120.90 (CH), 121.86 (CH), 122.38 (CH), 123.30 (CH), 125.44 (CH), 128.55 (CH), 129.57 (CH), 130.01 (C), 134.19 (CH), 137.05 (C), 138.30

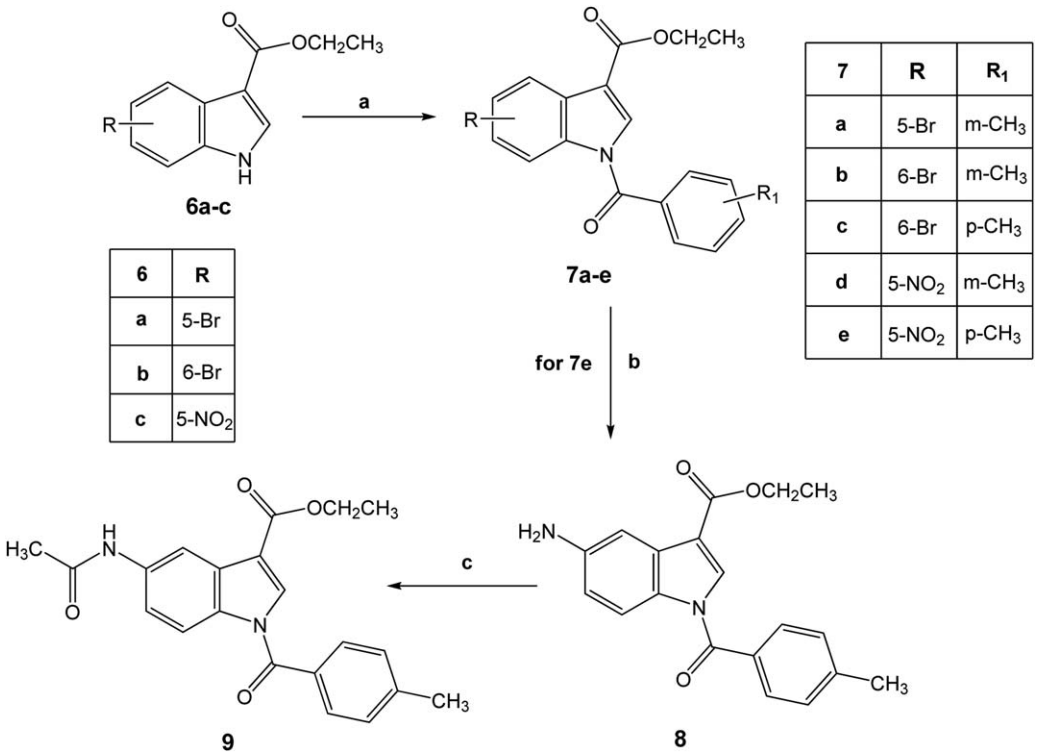

6	R
a	5-Br
b	6-Br
c	5-NO_2

7	R	R_1
a	5-Br	m-CH_3
b	6-Br	m-CH_3
c	6-Br	p-CH_3
d	5-NO_2	m-CH_3
e	5-NO_2	p-CH_3

Fig. 4. Synthesis of the final compounds **7a-e**, **8** and **9**. Reagents and conditions: a) NaH-I, *m*-o p-toluoyl chloride, anhydrous THF, r.t., 24 h; b) H_2, Pd/C, EtOH 96%. 30 PSI (Parr), 2 h; c) CH_3COCl. Et_3N, anhydrous CH_2Cl_2, 0°C, 2 h; r.t., 2 h.

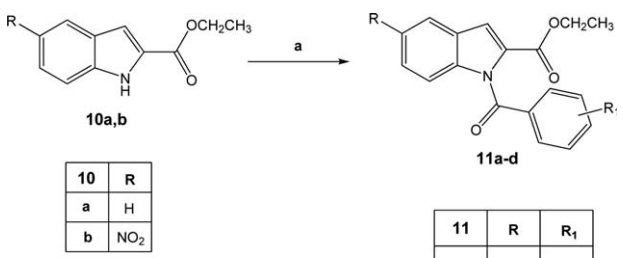

10	R
a	H
b	NO_2

11	R	R_1
a	H	m-CH_3
b	H	p-CH_3
c	NO_2	m-CH_3
d	NO_2	p-CH_3

Fig. 5. Synthesis of the final compounds **11a-d**. Reagents and conditions: a) NaH, *m*-o p-toluoyl chloride, anhydrous THF, r.t., 24 h.

(C), 140.33 (C). ESI-MS calcd. for $C_{18}H_{17}NO_2$, 279.33; found: *m/z* 280.13 $[M + H]^+$. Anal. $C_{18}H_{17}NO_2$ (C, H, N).

Ethyl 1-(3-methylbenzyl)-1H-indole-3-carboxylate (2b)

A mixture of ethyl 1H-indole-3-carboxylate **1a** (0.47 mmol), K_2CO_3 (0.94 mmol) and 3-methylbenzyl chloride (0.71 mmol) in 2 mL of anhydrous acetonitrile was stirred at reflux for 3 h. After cooling, the mixture was concentrated *in vacuo*, diluted with ice-cold water (10 mL), and extracted with ethyl acetate (3 x 15 mL). The organic phase was dried over sodium sulfate, and the solvent was evaporated in vacuo to obtain the final compound **2b**, which was purified by column chromatography using toluene/ethyl acetate (9.5:0.5) as eluent. Yield = 66%; oil. ^1H NMR ($CDCl_3$) δ 1.45 (t, 3H, OCH_2CH_3, J = 7.0 Hz), 2.33 (s, 3H, CH_3), 4.42 (q, 2H, OCH_2CH_3, J = 7.0 Hz), 5.31 (s, 2H, CH_2), 6.97-7.02 (m, 2H, Ar), 7.13 (d, 1H, Ar, J = 7.2 Hz), 7.22-7.36 (m, 4H, Ar), 7.88 (s, 1H, Ar), 8.23 (dd, 1H, Ar, J = 6.8 Hz, J = 1.2 Hz). ^{13}C NMR ($CDCl_3$) δ 13.60 (CH_3), 21.20 (CH_3), 59.10 (CH_2), 61.80 (CH_2), 102.05 (C), 111.07 (CH), 120.14 (CH), 121.03 (CH), 122.00 (CH), 126.24 (CH), 126.30 (CH), 128.05 (CH), 128.10 (C), 128.31 (CH), 129.97 (CH), 137.60 (C), 137.73 (C), 139.00 (C), 167.05 (C). ESI-MS calcd. for $C_{19}H_{19}NO_2$, 293.36; found: *m/z* 294.14 $[M + H]^+$. Anal. $C_{19}H_{19}NO_2$ (C, H, N).

General procedure for compounds (2c-g)

To a suspension of the substrate **1a** (0.53 mmol) in 10 mL of anhydrous THF, 1.06 mmol of sodium hydride and 0.64 mmol of appropriate benzoyl chloride were added. The mixture was stirred at room temperature overnight. The solvent was concentrated

in vacuo to obtain a residue that was purified by crystallization from ethanol.

Ethyl 1-(3-methylbenzoyl)-1H-indole-3-carboxylate (2c)

Yield = 23%; mp = 74-76°C (EtOH). ^{1}H NMR ($CDCl_3$) δ 1.43 (t, 3H, OCH_2CH_3, J = 7.2 Hz), 2.49 (s, 3H, CH_3), 4.42 (q, 2H, OCH_2CH_3, J = 7.2 Hz), 7.42-7.50 (m, 4H, Ar), 7.55 (d, 1H, Ar, J = 6.8 Hz), 7.60 (s, 1H, Ar), 8.02 (s, 1H, Ar), 8.22 (d, 1H, Ar, J = 8.4 Hz), 8.39 (d, 1H, Ar, J = 8.0 Hz). ^{13}C NMR ($CDCl_3$) δ 13.60 (CH_3), 20.50 (CH_3), 59.10 (CH_2), 102.00 (C), 111.06 (CH), 120.13 (CH), 121.08 (CH), 122.01 (CH), 124.00 (CH), 126.75 (CH), 128.02 (C), 128.96 (CH), 130.43 (CH), 135.00 (CH), 136.11 (C), 136.64 (C), 138.19 (C), 167.11 (C), 190.01 (C). ESI-MS calcd. for $C_{19}H_{17}NO_3$, 307.34; found: *m/z* 308.12 $[M + H]^+$. Anal. $C_{19}H_{17}NO_3$ (C, H, N).

Ethyl 1-(4-methylbenzoyl)-1H-indole-3-carboxylate (2d)

Yield = 74%; mp = 109-111°C (EtOH). ^{1}H NMR ($CDCl_3$) δ 1.40 (t, 3H, OCH_2CH_3, J = 7.0 Hz), 2.48 (s, 3H, CH_3), 4.39 (q, 2H, OCH_2CH_3, J = 7.0 Hz), 7.36 (d, 2H, Ar, J = 7.6 Hz), 7.40-7.45 (m, 2H, Ar), 7.66 (d, 2H, Ar, J = 8.0 Hz), 8.02 (s, 1H, Ar), 8.19 (d, 1H, Ar, J = 6.4 Hz), 8.34 (d, 1H, Ar, J = 6.4 Hz). ^{13}C NMR ($CDCl_3$) δ 14.45 (CH_3), 21.71 (CH_3), 60.50 (CH_2), 102.02 (C), 111.06 (CH), 116.13 (CH), 121.71 (CH), 124.85 (CH), 125.56 (CH), 128.00 (CH), 128.10 (C), 129.57 (CH), 129.73 (CH), 133.52 (CH), 133.70 (C), 136.04 (C), 143.65 (C), 167.01 (C), 190.00 (C). ESI-MS calcd. for $C_{19}H_{17}NO_3$, 307.34; found: *m/z* 308.12 $[M + H]^+$. Anal. $C_{19}H_{17}NO_3$ (C, H, N).

Ethyl 1-(4-chlorobenzoyl)-1H-indole-3-carboxylate (2e)

Yield = 89%; mp = 123-125°C (EtOH). ^{1}H NMR ($CDCl_3$) δ 1.44 (t, 3H, OCH_2CH_3, J = 7.2 Hz), 4.42 (q, 2H, OCH_2CH_3, J = 7.2 Hz), 7.45-7.50 (m, 2H, Ar), 7.58 (d, 2H, Ar, J = 8.4 Hz), 7.74 (d, 2H, Ar, J = 8.4 Hz), 7.97 (s, 1H, Ar), 8.10 (d, 2H, Ar, J = 8.8 Hz). ^{13}C NMR ($CDCl_3$) δ 14.11 (CH_3), 60.90 (CH_2), 108.62 (C), 115.66 (CH), 119.83 (CH), 121.81 (CH), 124.35 (CH), 124.39 (CH), 126.36 (C), 129.30 (CH), 129.38 (CH), 131.10 (C), 131.33 (CH), 131.37 (CH), 135.72 (C), 140.10 (C), 162.54 (C), 167.71 (C). ESI-MS calcd. for $C_{18}H_{14}ClNO_3$, 327.76; found: *m/z* 329.06 $[M + H]^+$. Anal. $C_{18}H_{14}ClNO_3$ (C, H, N).

Ethyl 1-(3-chlorobenzoyl)-1H-indole-3-carboxylate (2f)

Yield = 30%; mp = 89-91°C (EtOH). ^{1}H NMR ($CDCl_3$) δ 1.44 (t, 3H, OCH_2CH_3, J = 7.2 Hz), 4.43 (q, 2H, OCH_2CH_3, J = 7.2 Hz), 7.45-7.50 (m, 2H, Ar), 7.54 (t, 2H, Ar, J = 8.0 Hz), 7.63-7.68 (m, 2H, Ar), 7.78 (s, 1H, Ar), 7.95 (s, 1H, Ar), 8.06 (d, 1H, Ar, J = 7.6 Hz). ^{13}C NMR ($CDCl_3$) δ 14.19 (CH_3), 60.95 (CH_2), 108.66 (C), 115.60 (CH), 119.89 (CH), 121.84 (CH), 124.31 (CH), 124.35 (CH), 126.36 (C), 129.20 (CH), 129.98 (CH), 130.60 (CH), 131.93 (C), 134.67 (CH), 134.82 (C), 135.70 (C), 162.54 (C), 167.73 (C). ESI-MS calcd. for $C_{18}H_{14}ClNO_3$, 327.76; found: *m/z* 329.06 $[M + H]^+$. Anal. $C_{18}H_{14}ClNO_3$ (C, H, N).

Ethyl 1-(4-fluorobenzoyl)-1H-indole-3-carboxylate (2g)

Yield = 89%; mp = 123-125°C (EtOH). ^{1}H NMR ($CDCl_3$) δ 1.49 (t, 3H, OCH_2CH_3, J = 7.2 Hz), 4.45 (q, 2H, OCH_2CH_3, J = 7.2 Hz), 7.25 (t, 2H, Ar, J = 8.0 Hz), 7.48-7.53 (m, 2H, Ar), 7.70-7.75 (m, 2H, Ar), 8.01 (s, 1H, Ar), 8.15-8.20 (m, 2H, Ar). ^{13}C NMR ($CDCl_3$) δ 14.12 (CH_3), 60.94 (CH_2), 108.62 (C), 115.61 (CH), 116.03 (CH), 116.07 (CH), 119.55 (CH), 121.89 (CH), 124.33 (CH), 124.39 (CH), 126.38 (C), 128.60 (C), 131.53 (CH), 131.57 (CH), 135.72 (C), 162.50 (C), 167.74 (C), 168.71 (C). ESI-MS calcd. for $C_{18}H_{14}FNO_3$, 311.31; found: *m/z* 312.10 $[M + H]^+$. Anal. $C_{18}H_{14}FNO_3$ (C, H, N).

General procedure for compounds (3a,b)

Compounds **3a,b** were obtained following the same procedure performed for compounds **2c-g** and starting from intermediate **1b**. The final compounds **3a,b** were purified by column chromatography using cyclohexane/ethyl acetate (6:1) as eluent.

Ethyl 2-(1-(3-methylbenzoyl)-1H-indol-3-yl)acetate (3a)

Yield = 14%; oil. ^{1}H NMR ($CDCl_3$) δ 1.24 (t, 3H, OCH_2CH_3, J = 7.2 Hz), 2.44 (s, 3H, CH_3), 3.68 (s, 2H, CH_2), 4.16 (q, 2H, OCH_2CH_3, J = 7.2 Hz), 7.30 (s, 1H, Ar), 7.33-7.40 (m, 4H, Ar), 7.48-7.58 (m, 3H, Ar), 8.39 (d, 1H, Ar, J = 8.0 Hz). ^{13}C NMR ($CDCl_3$) δ 14.19 (CH_3), 21.38 (CH_3), 31.17 (CH_2), 61.08 (CH_2), 114.50 (C), 116.58 (CH), 119.03 (CH), 123.86 (CH), 125.22 (CH), 126.10 (CH), 126.17 (CH), 128.42 (CH), 129.59 (CH), 130.51 (C), 132.60 (CH), 134.60 (C), 136.24 (C), 138.63 (C), 168.72 (C), 170.79 (C). ESI-MS calcd. for $C_{20}H_{19}NO_3$, 321.37;

found: *m/z* 322.14 $[M + H]^+$. Anal. $C_{20}H_{19}NO_3$ (C, H, N).

Ethyl 2-(1-(4-methylbenzoyl)-1H-indol-3-yl)acetate (3b)

Yield = 37%; mp = 63-65°C (EtOH). ^{1}H NMR ($CDCl_3$) δ 1.25 (t, 3H, OCH_2CH_3, J = 7.0 Hz), 2.46 (s, 3H, CH_3), 3.69 (s, 2H, CH_2), 4.17 (q, 2H, OCH_2CH_3, J = 7.0 Hz), 7.31-7.41 (m, 5H, Ar), 7.57 (d, 1H, Ar, J = 7.6 Hz), 7.64 (d, 2H, Ar, J = 8.0 Hz), 8.38 (d, 1H, Ar, J = 8.0 Hz). ^{13}C NMR ($CDCl_3$) δ 14.20 (CH_3), 21.65 (CH_3), 31.13 (CH_2), 61.09 (CH_2), 114.31 (C), 116.51 (CH), 119.00 (CH), 123.78 (CH), 125.16 (CH), 126.18 (CH), 129.26 (CH), 129.27 (CH), 129.37 (CH), 129.38 (CH), 130.45 (C), 131.67 (C), 136.25 (C), 142.59 (C), 168.57 (C), 170.85 (C). ESI-MS calcd. for $C_{20}H_{19}NO_3$, 321.37; found: *m/z* 322.14 $[M + H]^+$. Anal. $C_{20}H_{19}NO_3$ (C, H, N).

General procedure for compounds (5a-g)

To a cooled (0°C) suspension of the substrate **1d** (0.40 mmol) in anhydrous CH_2Cl_2 (2 mL), Et_3N (0.10 mmol) and 1.15 mmol of the appropriate benzoyl chloride (for compounds **5a-e**) or sulfonyl chloride (for compounds **5f,g**) were added. The solution was stirred at 0°C for 2 h and then at room temperature for 2 h. After evaporation of the solvent, ice-cold water (20 mL) was added, and the mixture was neutralized with 0.5 N NaOH. Compounds **5a,b,e** were recovered by extraction with CH_2Cl_2 (3 x 15 mL), while all other compounds were recovered by vacuum filtration. The final compounds **5a-g** were purified by crystallization from ethanol.

1-(4-chlorobenzoyl)-N-phenyl-1H-indole-3-carboxamide (5a)

Yield = 60%; mp = 171-173°C (EtOH). ^{1}H NMR ($CDCl_3$) δ 7.18 (t, 1H, Ar, J = 7.4 Hz), 7.39 (t, 2H, Ar, J = 7.8 Hz), 7.45-7.50 (m, 2H, Ar), 7.55 (d, 2H, Ar, J = 8.8 Hz), 7.64 (d, 2H, Ar, J = 7.6 Hz), 7.72 (d, 2H, Ar, J = 8.8 Hz), 7.88 (s, 1H, Ar), 8.08-8.13 (m, 1H, Ar), 8.33-8.38 (m, 1H, Ar). ^{13}C NMR ($CDCl_3$) δ 112.00 (C), 115.66 (CH), 119.83 (CH), 121.61 (CH), 121.67 (CH), 121.80 (CH), 124.35 (CH), 124.39 (CH), 126.36 (C), 128.03 (CH), 128.90 (CH), 128.95 (CH), 129.34 (CH), 129.39 (CH), 131.11 (C), 131.31 (CH), 131.36 (CH), 135.72 (C), 137.93 (C), 140.10 (C), 164.77 (C), 167.70 (C). ESI-MS calcd. for $C_{22}H_{15}ClN_2O_2$, 374.82; found: *m/z* 376.08 $[M + H]^+$. Anal. $C_{22}H_{15}ClN_2O_2$ (C, H, N).

1-(3-chlorobenzoyl)-N-phenyl-1H-indole-3-carboxamide (5b)

Yield = 58%; mp = 161-163°C (EtOH). ^{1}H NMR ($CDCl_3$) δ 7.18 (t, 1H, Ar, J = 7.2 Hz), 7.40 (t, 2H, Ar, J = 7.2 Hz), 7.49-7.55 (m, 3H, Ar), 7.60-7.65 (m, 4H, Ar), 7.73 (exch br s, 1H, NH), 7.78 (s, 1H, Ar), 7.88 (s, 1H, Ar), 8.11 (d, 1H, Ar, J = 8.0 Hz), 8.40 (d, 1H, Ar, J = 7.2 Hz). ^{13}C NMR ($CDCl_3$) δ 112.02 (C), 115.60 (CH), 119.85 (CH), 121.63 (CH), 121.68 (CH), 121.80 (CH), 124.34 (CH), 124.37 (CH), 126.31 (C), 128.03 (CH), 128.92 (CH), 128.96 (CH), 129.24 (CH), 129.99 (CH), 130.61 (CH), 131.91 (C), 134.66 (CH), 134.82 (C), 135.73 (C), 137.90 (C), 164.77 (C), 167.71 (C). ESI-MS calcd. for $C_{22}H_{15}ClN_2O_2$, 374.82; found: *m/z* 376.08 $[M + H]^+$. Anal. $C_{22}H_{15}ClN_2O_2$ (C, H, N).

1-(4-methylbenzoyl)-N-phenyl-1H-indole-3-carboxamide (5c)

Yield = 35%; mp = 150-151°C (EtOH). ^{1}H NMR ($CDCl_3$) δ 2.51 (s, 3H, CH_3), 7.19 (t, 1H, Ar, J = 7.4 Hz), 7.30-7.40 (m, 4H, Ar), 7.45-7.50 (m, 2H, Ar), 7.60-7.75 (m, 5H, 4H Ar + 1H NH), 7.96 (s, 1H, Ar), 8.08-8.13 (m, 1H, Ar), 8.34-8.39 (m, 1H, Ar). ^{13}C NMR ($CDCl_3$) δ 21.30 (CH_3), 112.05 (C), 115.64 (CH), 119.83 (CH), 121.62 (CH), 121.68 (CH), 121.85 (CH), 124.35 (CH), 124.38 (CH), 126.31 (C), 128.04 (CH), 128.90 (CH), 128.96 (CH), 129.54 (CH), 129.59 (CH), 129.81 (CH), 129.85 (CH), 130.06 (C), 135.72 (C), 137.95 (C), 144.20 (C), 164.75 (C), 167.71 (C). ESI-MS calcd. for $C_{23}H_{18}N_2O_2$, 354.40; found: *m/z* 355.14 $[M + H]^+$. Anal. $C_{23}H_{18}N_2O_2$ (C, H, N).

1-(4-fluorobenzoyl)-N-phenyl-1H-indole-3-carboxamide (5d)

Yield = 77%; mp = 218-220°C (EtOH). ^{1}H NMR ($CDCl_3$) δ 7.19 (t, 1H, Ar, J = 7.2 Hz), 7.28 (t, 2H, Ar, J = 7.8 Hz), 7.39 (t, 2H, Ar, J = 8.0 Hz), 7.46-7.52 (m, 2H, Ar), 7.65 (d, 2H, Ar, J = 8.0 Hz), 7.71 (exch br s, 1H, NH), 7.80-7.85 (m, 2H, Ar), 7.92 (s, 1H, Ar), 8.10-8.15 (m, 1H, Ar), 8.34-8.39 (m, 1H, Ar). ^{13}C NMR ($CDCl_3$) δ 112.03 (C), 115.65 (CH), 116.03 (CH), 116.07 (CH), 119.88 (CH), 121.65 (CH), 121.69 (CH), 121.88 (CH), 124.31 (CH), 124.34 (CH), 126.30 (C), 128.06 (CH), 128.64 (C), 128.92 (CH), 128.96 (CH), 131.53 (CH), 131.56 (CH), 135.75 (C), 137.96 (C), 164.75 (C), 167.71 (C), 168.70 (C). ESI-MS calcd. for $C_{22}H_{15}FN_2O_2$, 358.37; found: *m/z* 359.12 $[M + H]^+$. Anal. $C_{22}H_{15}FN_2O_2$ (C, H, N).

1-(3-fluorobenzoyl)-N-phenyl-1H-indole-3-carboxamide (5e)

Yield = 30%; mp = 164-167°C (EtOH). ^{1}H NMR ($CDCl_3$) δ 7.19 (t, 1H, Ar, J = 7.2 Hz), 7.40 (t, 3H, Ar, J = 7.6 Hz), 7.50-7.60 (m, 5H, Ar), 7.64 (d, 2H, Ar, J = 8.0 Hz), 7.71 (exch br s, 1H, NH), 7.89 (s, 1H, Ar), 8.09-8.14 (m, 1H, Ar), 8.39-8.44 (m, 1H, Ar). ^{13}C NMR ($CDCl_3$) δ 112.05 (C), 114.75 (CH), 115.63 (CH), 119.87 (CH), 121.38 (CH), 121.65 (CH), 121.69 (CH), 121.80 (CH), 124.33 (CH), 124.38 (CH), 126.35 (C), 126.76 (CH), 128.04 (CH), 128.93 (CH), 128.97 (CH), 130.83 (CH), 132.16 (C), 135.70 (C), 137.95 (C), 163.45 (C), 164.71 (C), 167.70 (C). ESI-MS calcd. for $C_{22}H_{15}FN_2O_2$, 358.37; found: *m/z* 359.12 $[M + H]^+$. Anal. $C_{22}H_{15}FN_2O_2$ (C, H, N).

N-phenyl-1-tosyl-1H-indole-3-carboxamide (5f)

Yield = 64%; mp = 219-221°C (EtOH). ^{1}H NMR ($CDCl_3$) δ 2.39 (s, 3H, CH_3), 7.19 (t, 1H, Ar, J = 7.2 Hz), 7.30-7.45 (m, 5H, Ar), 7.60-7.70 (m, 3H, Ar), 7.85 (d, 2H, Ar, J = 7.2 Hz), 8.02 (d, 1H, Ar, J = 8.0 Hz), 8.12 (d, 1H, Ar, J = 7.6 Hz), 8.15 (s, 1H, Ar). ^{13}C NMR ($CDCl_3$) δ 21.35 (CH_3), 112.00 (C), 114.54 (CH), 119.89 (CH), 121.63 (CH), 121.69 (CH), 121.85 (CH), 124.95 (CH), 126.38 (C), 127.31 (CH), 128.04 (CH), 128.20 (CH), 128.26 (CH), 128.94 (CH), 128.99 (CH), 130.01 (CH), 130.05 (CH), 134.86 (C), 135.82 (C), 137.95 (C), 139.40 (C), 164.75 (C). ESI-MS calcd. for $C_{22}H_{18}N_2O_3S$, 390.45; found: *m/z* 391.11 $[M + H]^+$. Anal. $C_{22}H_{18}N_2O_3S$ (C, H, N).

1-((4-chlorophenyl)sulfonyl)-N-phenyl-1H-indole-3-carboxamide (5g)

Yield = 67%; mp = 216-218°C (EtOH). ^{1}H NMR ($CDCl_3$) δ 7.20 (t, 1H, Ar, J = 7.4 Hz), 7.40-7.50 (m, 7H, Ar), 7.60-7.70 (m, 2H, 1H Ar + 1H NH), 7.89 (d, 2H, Ar, J = 8.8 Hz), 8.01 (d, 1H, Ar, J = 7.6 Hz), 8.13 (s, 2H, Ar). ^{13}C NMR ($CDCl_3$) δ 112.01 (C), 114.53 (CH), 119.80 (CH), 121.61 (CH), 121.66 (CH), 121.85 (CH), 124.97 (CH), 126.35 (C), 127.31 (CH), 128.05 (CH), 128.91 (CH), 128.96 (CH), 129.74 (CH), 129.79 (CH), 129.81 (CH), 129.85 (CH), 135.86 (C), 135.92 (C), 137.95 (C), 139.30 (C), 164.71 (C). ESI-MS calcd. for $C_{21}H_{15}ClN_2O_3S$, 410.87; found: *m/z* 412.05 $[M + H]^+$. Anal. $C_{21}H_{15}ClN_2O_3S$ (C, H, N).

General procedure for compounds 7a-e

Compounds **7a-e** were obtained following the same procedure performed for compounds **2c-g** and **3a,b**, starting from intermediates **6a-c**. The final compounds **7a-e** were purified by crystallization from ethanol.

Ethyl 5-bromo-1-(3-methylbenzoyl)-1H-indole-3-carboxylate (7a)

Yield = 53%; mp = 136-137°C (EtOH). ^{1}H NMR ($CDCl_3$) δ 1.40 (t, 3H, OCH_2CH_3, J = 7.2 Hz), 2.46 (s, 3H, CH_3), 4.40 (q, 2H, OCH_2CH_3, J = 7.2 Hz), 7.42-7.56 (m, 5H, Ar), 7.98 (s, 1H, Ar), 8.23 (d, 1H, Ar, J = 8.8 Hz), 8.33 (d, 1H, Ar, J = 2.0 Hz). ^{13}C NMR ($CDCl_3$) δ 14.10 (CH_3), 23.90 (CH_3), 60.90 (CH_2), 108.70 (C), 113.36 (CH), 117.03 (C), 121.10 (CH), 121.21 (CH), 124.40 (CH), 126.95 (CH), 128.32 (C), 129.20 (CH), 130.23 (CH), 130.50 (C), 134.71 (C), 134.80 (CH), 138.90 (C), 166.01 (C), 167.81 (C). ESI-MS calcd. for $C_{19}H_{16}BrNO_3$, 386.24; found: *m/z* 387.03 $[M + H]^+$. Anal. $C_{19}H_{16}BrNO_3$ (C, H, N).

Ethyl 6-bromo-1-(3-methylbenzoyl)-1H-indole-3-carboxylate (7b)

Yield = 62%; oil. ^{1}H NMR ($CDCl_3$) δ 1.38 (t, 3H, OCH_2CH_3, J = 7.2 Hz), 2.46 (s, 3H, CH_3), 4.37 (q, 2H, OCH_2CH_3, J = 7.2 Hz), 7.41-7.55 (m, 5H, Ar), 7.94 (s, 1H, Ar), 8.02 (d, 1H, Ar, J = 8.4 Hz), 8.57 (d, 1H, Ar, J = 1.6 Hz). ^{13}C NMR ($CDCl_3$) δ 14.42 (CH_3), 21.38 (CH_3), 60.58 (CH_2), 113.32 (C), 119.30 (CH), 120.09 (C), 122.83 (CH), 126.55 (CH), 128.21 (CH), 128.76 (CH), 129.92 (CH), 132.91 (C), 133.44 (CH), 133.64 (CH), 136.94 (C), 139.10 (C), 144.00 (C), 163.67 (C), 168.59 (C). ESI-MS calcd. for $C_{19}H_{16}BrNO_3$, 386.24; found: *m/z* 387.03 $[M + H]^+$. Anal. $C_{19}H_{16}BrNO_3$ (C, H, N).

Ethyl 6-bromo-1-(4-methylbenzoyl)-1H-indole-3-carboxylate (7c)

Yield = 44%; mp > 300°C (EtOH). ^{1}H NMR ($CDCl_3$) δ 1.39 (t, 3H, OCH_2CH_3, J = 7.2 Hz), 2.48 (s, 3H, CH_3), 4.38 (q, 2H, OCH_2CH_3, J = 7.0 Hz), 7.37 (d, 2H, Ar, J = 8.0 Hz), 7.52 (dd, 1H, Ar, J = 8.6 Hz, J = 1.8 Hz), 7.65 (d, 2H, Ar, J = 8.0 Hz), 7.97 (s, 1H, Ar), 8.04 (d, 1H, Ar, J = 8.4 Hz), 8.57 (d, 1H, Ar, J = 1.2 Hz). ^{13}C NMR ($CDCl_3$) δ 14.43 (CH_3), 21.75 (CH_3), 60.68 (CH_2), 113.20 (C), 119.27 (CH), 119.43 (C), 122.85 (CH), 126.54 (C), 128.22 (CH), 129.67 (CH), 129.76 (CH), 129.99 (C), 130.65 (CH), 133.45 (CH), 133.70 (CH), 137.02 (C), 143.99 (C), 163.79 (C), 168.43 (C). ESI-MS calcd. for $C_{19}H_{16}BrNO_3$, 386.24; found: *m/z* 387.03 $[M + H]^+$. Anal. $C_{19}H_{16}BrNO_3$ (C, H, N).

Ethyl 1-(3-methylbenzoyl)−5-nitro-1H-indole-3-carboxylate (7d)

Yield = 93%; mp = 153-155°C (EtOH). ^{1}H NMR ($CDCl_3$) δ 1.44 (t, 3H, OCH_2CH_3, J = 7.2 Hz), 2.47 (s, 3H, CH_3), 4.44 (q, 2H, OCH_2CH_3, J = 7.2 Hz), 7.46-7.55 (m, 3H, Ar), 7.59 (s, 1H, Ar), 8.15 (s, 1H, Ar), 8.32 (dd, 1H, Ar, J = 9.2 Hz, J = 2.4 Hz), 8.46 (d, 1H, Ar, J = 9.2 Hz), 9.08 (d, 1H, Ar, J = 2.0 Hz). ^{13}C NMR ($CDCl_3$) δ 14.42 (CH_3), 21.41 (CH_3), 61.13 (CH_2), 113.97 (C), 116.54 (CH), 118.17 (CH), 120.77 (CH), 126.74 (CH), 127.71 (C), 128.97 (CH), 130.11 (CH), 132.24 (C), 134.28 (CH), 135.79 (CH), 139.25 (C), 139.38 (C), 145.16 (C), 163.11 (C), 167.51 (C). ESI-MS calcd. for $C_{19}H_{16}N_2O_5$, 352.34; found: m/z 353.11 $[M + H]^+$. Anal. $C_{19}H_{16}N_2O_5$ (C, H, N).

Ethyl 1-(4-methylbenzoyl)−5-nitro-1H-indole-3-carboxylate (7e)

Yield = 95%; mp = 176-178°C (EtOH). ^{1}H NMR ($CDCl_3$) δ 1.44 (t, 3H, OCH_2CH_3, J = 7.2 Hz), 2.50 (s, 3H, CH_3), 4.44 (q, 2H, OCH_2CH_3, J = 7.2 Hz), 7.40 (d, 2H, Ar, J = 8.0 Hz), 7.69 (d, 2H, Ar, J = 8.0 Hz), 8.17 (s, 1H, Ar), 8.31 (dd, 1H, Ar, J = 9.2 Hz, J = 2.4 Hz), 8.43 (d, 1H, Ar, J = 9.2 Hz), 9.08 (d, 1H, Ar, J = 2.4 Hz). ^{13}C NMR ($CDCl_3$) δ 14.12 (CH_3), 21.31 (CH_3), 60.93 (CH_2), 108.60 (C), 112.04 (CH), 115.07 (CH), 116.00 (CH), 124.34 (CH), 127.21 (C), 129.50 (CH), 129.81 (CH), 130.04 (C), 132.28 (C), 134.25 (CH), 135.70 (CH), 141.89 (C), 144.25 (C), 162.50 (C), 167.71 (C). IR = 1332-1558 cm^{-1} (NO_2), 1690 cm^{-1} (C = O amide), 1710 cm^{-1} (C = O ester). ESI-MS calcd. for $C_{19}H_{16}N_2O_5$, 352.34; found: m/z 353.11 $[M + H]^+$. Anal. $C_{19}H_{16}N_2O_5$ (C, H, N).

Ethyl 5-amino-1-(4-methylbenzoyl)−1H-indole-3-carboxylate (8)

Compound **7e** (1.42 mmol) was reduced in Parr instrument (27 mL EtOH, 320 mg 10% Pd/C, 30 psi, 2 h). The catalyst was filtered off, and the solvent was evaporated under vacuum, resulting in the final compound, which was purified by column chromatography using cyclohexane/ethyl acetate (1:1) as eluent. Yield = 26%; mp = 152-154°C (EtOH). ^{1}H NMR (DMSO-d_6) δ 1.26 (t, 3H, OCH_2CH_3, J = 7.2 Hz), 2.40 (s, 3H, CH_3), 4.23 (q, 2H, OCH_2CH_3, J = 7.2 Hz), 5.21 (exch br s, 2H, NH_2), 6.69 (d, 1H, Ar, J = 8.4 Hz), 7.24 (s, 1H, Ar), 7.39 (d, 2H, Ar, J = 8.0 Hz), 7.63-7.68 (m, 3H, Ar), 7.93 (d, 1H, Ar, J = 8.6 Hz). ^{13}C NMR (DMSO-d_6) δ 14.10 (CH_3), 21.31 (CH_3), 60.95 (CH_2), 104.60 (CH), 108.64 (C), 107.37 (CH), 111.90 (CH), 124.34 (CH), 125.71 (C), 126.90 (C), 127.61 (C), 129.54 (CH), 129.88 (CH), 134.25 (CH), 135.73 (CH), 143.99 (C), 144.25 (C), 162.56 (C), 167.70 (C). IR = 1689 cm^{-1} (C = O amide), 1710 cm^{-1} (C = O ester), 3356-3460 cm^{-1} (NH_2). ESI-MS calcd. for $C_{19}H_{18}N_2O_3$, 322.36; found: m/z 323.14 $[M + H]^+$. Anal. $C_{19}H_{18}N_2O_3$ (C, H, N).

Ethyl 5-acetamido-1-(4-methylbenzoyl)−1H-indole-3-carboxylate (9)

Compound **9** was obtained starting from intermediate **8** and following the same procedure performed for compounds **5a-e** using acetyl chloride as reagent. Compound **9** was recovered by vacuum filtration and was purified by column chromatography using cyclohexane/ethyl acetate (1:2) as eluent. Yield = 15%; mp = 187-189°C dec. (EtOH). ^{1}H NMR (DMSO-d_6) δ 1.40 (t, 3H, OCH_2CH_3, J = 6.8 Hz), 2.22 (s, 3H, CH_3CONH), 2.47 (s, 3H, CH_3), 4.37 (q, 2H, OCH_2CH_3, J = 6.4 Hz), 7.35 (d, 2H, Ar, J = 7.6 Hz), 7.44 (exch br s, 1H, NH), 7.64 (d, 3H, Ar, J = 7.2 Hz), 7.99 (s, 1H, Ar), 8.23-8.28 (m, 2H, Ar). ^{13}C NMR (DMSO-d_6) δ 14.11 (CH_3), 21.30 (CH_3), 24.05 (CH_3), 60.90 (CH_2), 108.63 (C), 109.94 (CH), 111.37 (CH), 112.61 (CH), 124.30 (CH), 126.31 (C), 127.60 (C), 128.95 (CH), 129.51 (CH), 129.84 (CH), 130.11 (CH), 131.38 (C), 133.85 (C), 144.23 (C), 162.50 (C), 167.75 (C), 168.96 (C). ESI-MS calcd. for $C_{21}H_{20}N_2O_4$, 364.39; found: m/z 365.15 $[M + H]^+$. Anal. $C_{21}H_{20}N_2O_4$ (C, H, N).

General procedure for compounds (11a-d)

Compounds **11a-d** were obtained starting from intermediates **10a,b** and following the same procedure performed for compounds **2c-g**, **3a,b**, and **7a-e**. The final compounds **11a-d** were purified by column chromatography using toluene/ethyl acetate (9:1) (for **11a**) or cyclohexane/ethyl acetate (6:1) (for **11b-d**) as eluents.

Ethyl 1-(3-methylbenzoyl)−1H-indole-2-carboxylate (11a)

Yield = 4%; oil. ^{1}H NMR ($CDCl_3$) δ 1.08 (t, 3H, OCH_2CH_3, J = 7.2 Hz), 2.38 (s, 3H, CH_3), 3.97 (q, 2H, OCH_2CH_3, J = 7.2 Hz), 7.27-7.41 (m, 5H, Ar), 7.46 (d, 1H, Ar, J = 7.6 Hz), 7.56 (s, 1H, Ar), 7.70 (d, 1H, Ar, J = 8.0 Hz), 7.77 (d, 1H, Ar, J = 8.4 Hz). ^{13}C NMR ($CDCl_3$) δ 14.10 (CH_3), 20.95 (CH_3), 60.90 (CH_2), 108.42 (CH), 115.66 (CH), 119.83 (CH), 123.58 (CH), 124.31 (CH), 126.20 (C), 126.35 (C), 128.12 (CH), 129.16 (CH), 130.13 (CH), 130.40 (C), 134.81 (CH), 138.94 (C), 140.69 (C), 160.11 (C), 167.70 (C). ESI-MS calcd. for $C_{19}H_{17}NO_3$, 307.34;

found: *m/z* 308.12 $[M + H]^+$. Anal. $C_{19}H_{17}NO_3$ (C, H, N).

Ethyl 1-(4-methylbenzoyl)−1H-indole-2-carboxylate (11b)

Yield = 8%; oil. ^{1}H NMR ($CDCl_3$) δ 1.10 (t, 3H, OCH_2CH_3, J = 7.2 Hz), 2.41 (s, 3H, CH_3), 3.99 (q, 2H, OCH_2CH_3, J = 7.2 Hz), 7.23-7.30 (m, 3H, Ar), 7.35-7.40 (m, 2H, Ar), 7.61 (d, 2H, Ar, J = 8.4 Hz), 7.68-7.73 (m, 2H, Ar). ^{13}C NMR ($CDCl_3$) δ 14.10 (CH_3), 21.35 (CH_3), 60.92 (CH_2), 108.40 (CH), 115.68 (CH), 119.81 (CH), 123.55 (CH), 124.30 (CH), 126.25 (C), 126.31 (C), 129.52 (CH), 129.86 (CH), 130.03 (C), 130.40 (CH), 134.85 (CH), 140.64 (C), 144.20 (C), 160.10 (C), 167.75 (C). ESI-MS calcd. for $C_{19}H_{17}NO_3$, 307.34; found: *m/z* 308.12 $[M + H]^+$. Anal. $C_{19}H_{17}NO_3$ (C, H, N).

Ethyl 1-(3-methylbenzoyl)−5-nitro-1H-indole-2-carboxylate (11c)

Yield = 33%; mp = 123-125°C (EtOH). ^{1}H NMR ($CDCl_3$) δ 1.12 (t, 3H, OCH_2CH_3, J = 7.2 Hz), 2.40 (s, 3H, CH_3), 4.03 (q, 2H, OCH_2CH_3, J = 7.0 Hz), 7.35 (t, 1H, Ar, J = 7.6 Hz), 7.40-7.45 (m, 3H, Ar), 7.55 (s, 1H, Ar), 7.79 (d, 1H, Ar, J = 9.2 Hz), 8.26 (dd, 1H, Ar, J = 9.2 Hz, J = 2.4 Hz), 8.66 (d, 1H, Ar, J = 2.0 Hz). ^{13}C NMR ($CDCl_3$) δ 13.82 (CH_3), 21.27 (CH_3), 61.89 (CH_2), 114.18 (CH), 114.81 (CH), 119.21 (CH), 121.81 (CH), 126.73 (CH), 128.14 (C), 128.92 (CH), 130.06 (CH), 131.50 (C), 134.29 (C), 134.87 (CH), 139.17 (C), 141.02 (C), 144.08 (C), 160.15 (C), 168.30 (C). ESI-MS calcd. for $C_{19}H_{16}N_2O_5$, 352.34; found: *m/z* 353.11 $[M + H]^+$. Anal. $C_{19}H_{16}N_2O_5$ (C, H, N).

Ethyl 1-(4-methylbenzoyl)−5-nitro-1H-indole-2-carboxylate (11d)

Yield = 13%; mp = 109-111°C (EtOH). ^{1}H NMR ($CDCl_3$) δ 1.13 (t, 3H, OCH_2CH_3, J = 7.2 Hz), 2.44 (s, 3H, CH_3), 4.06 (q, 2H, OCH_2CH_3, J = 7.2 Hz), 7.28 (d, 2H, Ar, J = 8.0 Hz), 7.49 (s, 1H, Ar), 7.60 (d, 2H, Ar, J = 8.4 Hz), 7.73 (d, 1H, Ar, J = 9.2 Hz), 8.25 (dd, 1H, Ar, J = 9.2 Hz, J = 2.0 Hz), 8.66 (d, 1H, Ar, J = 2.0 Hz). ^{13}C NMR ($CDCl_3$) δ 13.85 (CH_3), 21.84 (CH_3), 61.88 (CH_2), 114.03 (CH), 114.76 (CH), 119.26 (CH), 121.71 (CH), 126.60 (C), 129.76 (CH), 129.77 (CH), 129.80 (CH), 129.81 (CH), 131.49 (C), 133.80 (C), 141.00 (C), 143.96 (C), 145.39 (C), 160.15 (C), 168.32 (C). ESI-MS calcd. for $C_{19}H_{16}N_2O_5$, 352.34; found: *m/z* 353.11 $[M + H]^+$. Anal. $C_{19}H_{16}N_2O_5$ (C, H, N).

Pharmacology

Compounds were dissolved in 100% DMSO at 5 mM stock concentrations. The final concentration of DMSO in the reactions was 1%, a level of DMSO that had no effect on enzyme activity. The HNE inhibition assay was performed in black flat-bottom 96-well microtiter plates. Briefly, a mixture of 200 mM Tris–HCl, pH 7.5, 0.01% bovine serum albumin (Fisher Scientific), 0.05% Tween-20, and 20 mU/mL of HNE (Calbiochem) was added to wells containing different concentrations of each compound. The reaction was initiated by addition of 25 μM elastase substrate (N-methylsuccinyl-Ala-Ala-Pro-Val-7-amino-4-methylcoumarin, Calbiochem) in a final reaction volume of 100 μL/well. Kinetic measurements were obtained every 30 s for 10 min at 25°C using a Fluoroskan Ascent FL fluorescence microplate reader (Thermo Electron, MA) with excitation and emission wavelengths at 355 and 460 nm, respectively. For all compounds tested, the concentration of inhibitor that caused 50% inhibition of the enzymatic reaction (IC_{50}) was calculated by plotting percentage inhibition versus log inhibitor concentration (a minimum of six points). The data were presented as the mean values of at least three independent experiments with relative standard deviations of less than 15%.

Molecular Modeling

Initial structures of the compounds **2c**, **4a**, **7d**, and **A1-A3** (Tables 1 and 2) were generated using HyperChem 8.0 (Shimadzu Corporation, Kyoto, Japan) and optimized by the semi-empirical PM3 method. Docking of the molecules was performed with the use of Molegro Virtual Docker, version 4.2.0 (CLC Bio, Copenhagen, Denmark) as described previously [Giovannoni et al., 2015]. The structure of HNE complexed with a peptide chloromethyl ketone inhibitor was used for the docking study (1HNE from the Protein Data Bank). The search area for docking poses was defined as a sphere with 10 Å radius centered at the nitrogen atom in the five-membered ring of the peptide chloromethyl ketone inhibitor. After removal of this peptide and co-crystallized water molecules from the program workspace, we set side chain flexibility for the 42 residues closest to the center of the search area as reported previously [Giovannoni et al., 2015]. These flexible residues included the catalytic triad of Ser195, His57, and Asp102. Fifteen docking runs were performed for each compound, with full flexibility of a ligand around all rotatable bonds and side chain flexibility of the above-mentioned residues of the enzyme. Parameters used within Docking Wizard of the

TABLE 1. HNE Inhibitory Activity of Indole Derivatives 2a-g, 3a,b, 4a,b, 5a-g

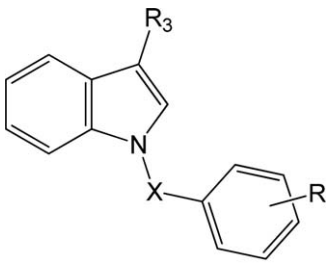

2a-g, 3a,b, 4a,b, 5a-g

Comp	R_3	X	R	IC_{50} (μM)[a]
2a	COOEt	-	m-CH_3	NA[b]
2b	COOEt	CH_2	m-CH_3	NA[b]
2c	COOEt	CO	m-CH_3	NA[b]
2d	COOEt	CO	p-CH_3	NA[b]
2e	COOEt	CO	p-Cl	3.8 ± 0.4
2f	COOEt	CO	m-Cl	NA[b]
2g	COOEt	CO	p-F	12.2 ± 2.3
3a	CH_2COOEt	CO	m-CH_3	NA[b]
3b	CH_2COOEt	CO	p-CH_3	NA[b]
4a	CN	CO	m-CH_3	NA[b]
4b	CN	CO	p-CH_3	10.1 ± 1.3
5a	CONHPh	CO	p-Cl	NA[b]
5b	CONHPh	CO	m-Cl	NA[b]
5c	CONHPh	CO	p-CH_3	45.3 ± 6.7
5d	CONHPh	CO	p-F	NA[b]
5e	CONHPh	CO	m-F	NA[b]
5f	CONHPh	SO_2	p-CH_3	NA[b]
5g	CONHPh	SO_2	p-Cl	NA[b]
A1[c]	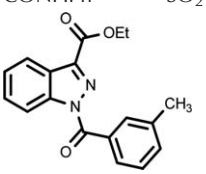			0.41 ± 0.11
A2[d]	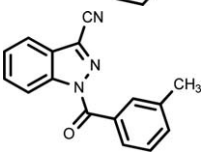			0.007 ± 0.0015

[a]IC_{50} values are presented as the mean ± SD of three independent experiments.
[b]NA: no inhibitory activity was found at the highest concentration of compound tested (50 μM).
[c]Crocetti et al., 2011.
[d]Crocetti et al., 2013.

Molegro program were as described previously [Giovannoni et al., 2015].

RESULTS AND DISCUSSION

All compounds were evaluated for their ability to inhibit HNE with the results are reported in

TABLE 2. HNE Inhibitory Activity of Indole Derivatives 7a-e, 8, and 9

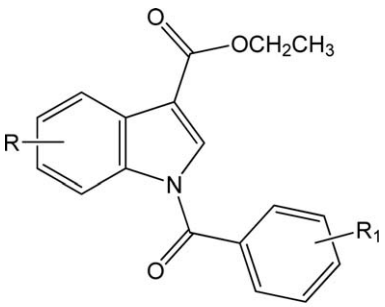

7a-e, 8, 9

Comp	R	R_1	IC_{50} (μM)[a]
7a	5-Br	m-CH_3	21.6 ± 3.3
7b	6-Br	m-CH_3	NA[b]
7c	6-Br	p-CH_3	10.5 ± 1.7
7d	5-NO_2	m-CH_3	2.4 ± 0.4
7e	5-NO_2	p-CH_3	13.2 ± 1.8
8	5-NH_2	p-CH_3	NA[b]
9	5-$NHCOCH_3$	p-CH_3	NA[b]
A3[c]	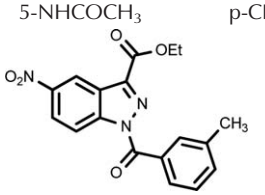		0.02 ± 0.028

[a]IC_{50} values are presented as the mean ± SD of three independent experiments.
[b]NA: no inhibitory activity was found at the highest concentration of compound tested (50 μM).
[c]Crocetti et al., 2013.

Tables (1–3) together with activity values of some potent *N*-benzoylindazoles (**A1-A3**) previously synthesized [Crocetti et al., 2011, 2013]. From a first evaluation of the biological data, it appeared evident that the indole nucleus was not as effective as the indazole nucleus for HNE inhibition, as the most active compounds had IC_{50} values in the micromolar range, and many of the synthesized compounds were inactive at the highest tested concentration of 50 μM. These results do, however, provide new information on the importance of various substituents in developing compounds with HNE inhibitor activity.

As shown in Table 1, the introduction of functions and groups (COOEt, CN, CONHPh) at position 3 of the indazole series resulted in several compounds with activity in the micromolar range (**2e, 2g**, **4b**, and **5c** with IC_{50} values of 3.8 μM, 12.2 μM, 10.1 μM, and 45.3 μM, respectively). All other compounds were inactive (IC_{50} values greater than 50 μM). Interestingly, we found opposite activities between the pairs of isomers **2e/2f** and **4a/4b**. In

TABLE 3. HNE Inhibitory Activity of Indole Derivatives 11a-d

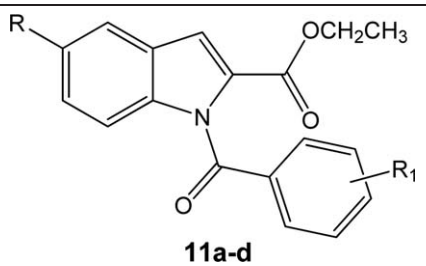

11a-d

Comp	R	R_1	IC_{50} (μM)[a]
11a	H	m-CH_3	NA[b]
11b	H	p-CH_3	NA[b]
11c	NO_2	m-CH_3	NA[b]
11d	NO_2	p-CH_3	NA[b]

[a]IC_{50} values are presented as the mean ± SD of three independent experiments.
[b]NA: no inhibitory activity was found at the highest concentration of compound tested (50 μM).

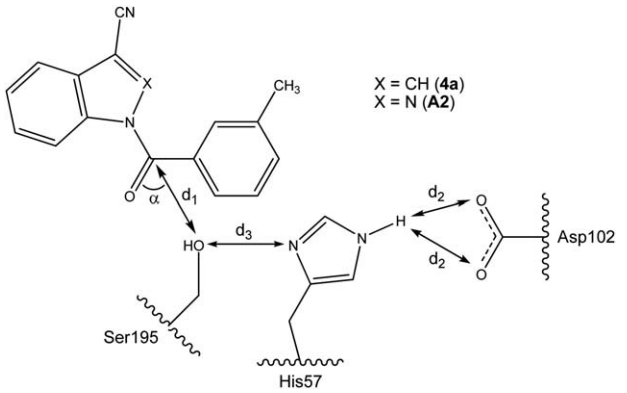

Fig. 6. Geometric parameters important for formation of a Michaelis complex in the HNE active site [an example is shown for compounds **4a** (X = CH) and **A2** (X = N)]. Based on the model of synchronous proton transfer from the oxyanion hole in HNE [Vergely et al., 1996; Peters and Merz, 2006].

both pairs, the derivative with the benzoyl fragment substituted in the *meta* position was inactive (i.e.,compounds **2f** and **4a**), whereas the corresponding *para*-substituted derivatives had appreciable activity. This trend was in contrast to that found for the indazole series, where both isomers were active [Crocetti et al., 2013]. Furthermore, inactive **4a** is the deaza analog of reference compound **A2**, which is the most potent HNE inhibitor we have synthesized to date (IC_{50} = 7 nM). Although compounds **2a**,**b** and **5f**,**g** were synthesized with the goal of confirming the importance of the carbonyl group at N-1, the lack of activity of these compounds suggests this molecular feature is not the point of attack of serine OH.

The introduction at position *5* or *6* of substituents that led to the best results in the previous series of compounds [Crocetti et al., 2013], such as nitro, bromine, and acetamido, led only to compounds with low HNE inhibitory activity (**7a**, IC_{50} = 21.6 μM; **7c**, IC_{50} = 10.5 μM; **7d**, IC_{50} = 2.4 μM; **7e**, IC_{50} = 13.2 μM) or no activity (**7b, 8** and **9**) (Table 2). The same results were found by moving the carbethoxy function from position *3* to position *2* (Table 3).

Docking studies showed that pairs of molecules differing in the presence or absence of pyrazole-type nitrogen atom in the five-membered heterocycle (**A1** vs. **2c** and **A2** vs. **4a**, respectively) exhibited differences in molecule orientation within the receptor cavity. However, molecules **A3** and **7d** had almost coinciding positions of the *m*-tolyl and heterocyclic moieties with the ester and amide fragments. According to the general catalytic mechanism of serine proteases, the ligand forms a Michaelis complex through attack of its electron-deficient atom (usually carbonyl carbon) at the Ser195 hydroxyl group. This complex formation is accompanied by the proton transfer from Ser195 to Asp102 via His57. Length **L** of the proton transfer channel is one of the factors influencing the interaction of a ligand with HNE. The other factor is the geometry of the Michaelis complex. It was reported earlier [Vergely et al., 1996; Peters and Merz, 2006] that the value of angle α between the C = O bond in the ligand and the Ser195···CO axis should lie within 80…120° for effective binding of the carbonyl group to Ser195 (Figure 6). Although docking poses are not identical for Michaelis complexes, the geometry of the poses can be used for the evaluation of complexation possibilities. Specifically, the amide carbonyl group was located in the vicinity of HNE Ser195 for all of the compounds evaluated in the docking study except for inhibitor **A1**, which has an ester carbonyl group orientation favorable for interaction with the catalytic triad (Ser195, His57, and Asp102).

The geometric characteristics of pose orientations and arrangements of the triad were in general agreement with the inhibitory activities of the compounds towards HNE (Table 4). Thus, the proton transfer channel had significantly shorter lengths for active compounds **A1** and **A2** (**L** value is between 5 and 6 Å) compared to their inactive indole counterparts **2c** and **4a**, respectively (**L** > 8 Å). HNE inhibitor **A3** had a geometry of the Ser195···C = O fragment more preferable for interaction with the catalytic triad than its less active indole analogue **7d**, which had a large angle α of 147°. Although the docking pose of **A3** was characterized by a slightly

TABLE 4. Biological Activities and Geometric Parameters of the Enzyme–Inhibitor Complexes Predicted by Molecular Docking

Comp	IC_{50} (μM)[a]	α	d_1	d_2	d_3	L[b]
A1[c]	0.4	84.8	2.529	2.361, 3.688	3.502	5.863
2c	NA	91.2	3.681	5.713, 5.989	2.454	8.167
A2	0.007	105.2	3.448	2.181, 3.755	3.142	5.323
4a	NA	78.5	3.936	5.756, 5.919	2.480	8.236
A3	0.02	116.9	4.078	3.056, 4.281	3.119	6.175
7d	2.4	147.0	4.260	2.828, 3.920	2.219	5.747

[a]HNE inhibitory activity.
[b]The length of the proton transfer channel was calculated as $L = d_3 + \min(d_2)$.
[c]According to the docking results, Michaelis complex with Ser195 is formed with participation of the ester carbonyl group.

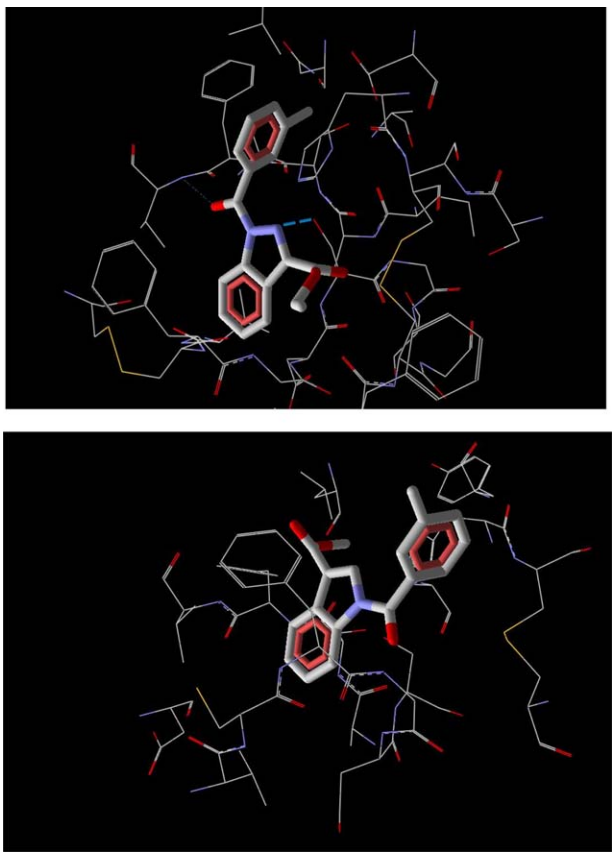

Fig. 7. Docking poses of HNE inhibitor **A1** (panel A) and compound **2c** (panel B). Ser195 of HNE is H-bonded with the pyrazole-type nitrogen of inhibitor **A1** (light-blue dashed line). Residues within 4 Å of the pose are shown. [Color figure can be viewed in the online issue, which is available at wileyonlinelibrary.com.]

higher **L** value than the pose for **7d**, the magnitude of α for **A3** fell into the optimum interval (Table 4).

We have found that the pyrazole-type nitrogen of indazoles forms H-bonds with Ser195 (inhibitor **A1**) or Gly193 (inhibitor **A2**) (see example in Figure 7). The carbonyl group in **A3** is strongly H-bonded to Val216, while the corresponding indole counterpart **7d** did not form H-bonds with HNE. Perhaps, these H-bonding interactions play an important role in the proper anchoring of inhibitors within the HNE binding site and can be used to explain differences in inhibitory properties of indazole and indole derivatives.

CONCLUSIONS

We found that the new indazole derivatives designed as deaza analogs of our potent N-benzoylindazoles are weak HNE inhibitors or even inactive. These results thus suggest the crucial role of the nitrogen at position 2 of the heterocyclic scaffold. The biological results are supported by docking studies, which highlighted the different orientation within the receptor cavity for indazoles and indoles with the former exhibiting H-bonding interactions favorable for interaction with the catalytic triad, while the latter were characterized by unfavorable anchoring.

REFERENCES

Bayer Corp: Prolastin. 2002. Company World Wide Web Site. Available at: http://www.bayerdirect.com/pro.htm/.

Bode W, Meyer E, Powers JC. 1989. Human leukocyte and porcine pancreatic elastase: X-ray crystal structures, mechanism, substrate specificity, and mechanism-based inhibitors. Biochemistry 28:1951–1963.

Cepinskas G, Sanding M, Kvietys PR. 1999. PAF-induced elastase-dependent neutrophil trans endothelial migration is associated with the mobilization of the elastase to the neutrophil surface and localization to the migration front. J Cell Sci 112:1937–1945.

Chua F, Laurent GJ. 2006. Neutrophil elastase: mediator of extracellular matrix destruction and accumulation. Proc Am Thorac Soc 3:424–427.

Crocetti L, Giovannoni MP, Schepetkin IA, Quinn MT, Khlebnikov AI, Cilibrizzi A, Dal Piaz V, Graziano A, Vergelli C. 2011. Design, synthesis and evaluation of N-benzoylindazole derivatives and analogues as inhibitors of human neutrophil elastase. Bioorg Med Chem 19:4460–4472.

Crocetti L, Schepetkin IA, Cilibrizzi A, Graziano A, Vergelli C, Giomi D, Khlebnikov AI, Quinn MT, Giovannoni MP. 2013. Optimization of N-benzoylindazole derivatives as inhibitors of human neutrophil elastase. J Med Chem 56:6259–6272.

DeGraw JI, Goodman L. 1964. Alkylating agents derived from indole-IV-synthesis of the 5-nitrogen mustard of indole-3-carboxylic acid. J Med Chem 7:213–215.

Geraghty P, Rogan MP, Greene CM, Boxio RMM, Poiriert T, O'Mahony M, Belaaouaj A, O'Neill SJ, Taggart CC, McElvaney NG. 2007. Neutrophil elastase up regulates cathepsin B and metalloproteinases-2 expression. J Immunol 178:5871–5878.

Gifford AM, Chalmers JD. 2014. The role of neutrophils in cystic fibrosis. Curr Opin Hematol 21:16–22.

Giovannoni MP, Schepetkin IA, Crocetti L, Ciciani G, Cilibrizzi A, Guerrini G, Khlebnikov AI, Quinn MT, Vergelli C. 2015. Cinnoline derivative as human neutrophil elastase inhibitors. J Enzym Inhib Med Chem 31:628–639.

Groutas WC, Dou D, Alliston KR. 2011. Neutrophil elastase inhibitors. Expert Opin Ther Pat 21:339–354.

Henriksen PA. 2014. The potential of neutrophil elastase inhibitors as anti-inflammatory therapies. Curr Opin Hematol 21:23–28.

Henrisken PA, Sallenave JM. 2008. Human neutrophil elastase: mediator target in atherosclerosis. Int J Biochem Cell B 40: 1095–1100.

Hermant B, Bibert S, Concord E, Dublet B, Wiedenhaup M, Vernet T, Gulino-Debrac D. 2003. Identification of proteases involved in the proteolysis of vascular endothelium cadherin during neutrophil transmigration. J Biol Chem 278:14002–14012.

Heutinck KM, Ten Berge IJ, Hack CE, Hamann J, Rowshani AT. 2010. Serine proteases of the human system in health and disease. Mol Immunol 47:1943–1955.

Hilbert N, Schiller J, Arnold J, Arnold K. 2002. Cartilage degradation by stimulated human neutrophils: elastase is mainly responsible for cartilage damage. Bioorg Chem 30:119–132.

Hogg JC, Chu F, Utokaparch S, Woods R, Elliott WM, Buzatu L, CherniacK RM, Rogers RM, Sciurba FC, Coxson HO, Parè PD. 2004. The nature of small-airway obstruction in chronic obstructive pulmonary disease. N Engl J Med 350:2645–2653.

Iwata K, Doi A, Ohji G, Oka H, Oba Y, Takimoto K, Igarashi W, Gremillion DH, Shimada T. 2010. Effect of neutrophil elastase inhibitors (sivelestat sodium) in the treatment of acute lung injury (ALI) and acute respiratory distress (ARDS): a systematic review and meta-analysis. Intern Med 49:2423–2432.

Kawabata K, Hagio T, Matsuoka S. 2002. The role of neutrophil elastase in acute lung injury. Eur J Pharmacol 451:1–10.

Korkmaz B, Horwitz MS, Jenne DE, Gauthier F. 2010. Neutrophil elastase, proteinase 3, and cathepsin G as therapeutic targets in human diseases. Pharmacol Rev 62:726–759.

Korkmaz B, Moreau T, Gauthier F. 2008. Neutrophil elastase, proteinase 3 and cathepsin G: physicochemical properties, activity and physiopathological functions. Biochimie 90:227–242.

Li LZ, Gao PY, Song SJ. 2012. Monoindole alkaloids from a marine sponge mycale fibrexilis. Biochem Syst Ecol 43:210–213.

Lucas SD, Costa E, Guedes RC, Moreira R. 2011. Targeting COPD: advances on low-molecular-weight inhibitors of human neutrophil elastase. Med Res Rev 33:E73–E101.

Meyer-Hoffert U, Wingertzahn J, Wiedow O. 2004. Human leukocyte elastase induces keratinocyte proliferation by epidermal growth factor receptor activation. J Invest Dermatol 123:338–345.

Moroy G, Alix AJ, Sapi J, Hornebeck W, Bourguet E. 2012. Neutrophil elastase as a target in lung cancer. Anticancer Agents Med Chem 12:565–579.

O'Donnell R, Peebles A, Ward C, Daraker A, Angco G, Broberg P, Pierrou S, Lund J, Holgate ST, Davies DE, et al. 2004. Relationship between peripheral airway dysfunction, airway obstruction and neutrophil inflammation in COPD. Thorax 59: 837–842.

Panatur N, Dalimbaa U, Koushikb PV, Alvalab M, Yogeeswarib P, Sriramb D, Kumarc V. 2013. Identification and characterization of novel indole based small molecules as anticancer agents through SIRT1 inhibition. Eur J Med Chem 69:125–138.

Perera NC, Schilling O, Kittel H, Back W, Kremmer E, Jenne DE. 2012. NSP4, an elastase-related protease in human neutrophils with arginine specificity. Proc Natl Acad Sci USA 109: 6229–6234.

Pham CT. 2006. Neutrophil serine proteases: specific regulators of inflammation. Nat Rev Immunol 6:541–550.

Peters MB, Merz KM. 2006. Semiempirical comparative binding energy analysis (SE-COMBINE) of a series of trypsin inhibitors. J Chem Theory Comput 2:383–399.

Potempa J, Korzus E, Travis J. 1994. The serpin superfamily of proteinase inhibitors: structure, function and regulation. J Biol Chem 269:15957–15960.

Reeves EP, Lu H, Jacobs HL, Messina CGM, Bolsover S, Gabella G, Potma EO, Warley A, Roes J, Segal AW. 2002. Killing activity of neutrophils is mediated through activation of proteases by K^+ flux. Nature 416:291–297.

Sato T, Takahashi S, Mizumoto T, Haraoc M, Akizukid M, Takasugid M, Fukutomid T, Yamashita J. 2006. Neutrophil elastase and cancer. Surg Oncol 15:217–222.

Semple BD, Trivedi A, Gimlin K, Noble-Haeusslein LJ. 2015. Neutrophil elastase mediates acute pathogenesis and is a determinant of long-term behavioral recovery after traumatic injury to the immature brain. Neurobiol Dis 74:263–280.

Shahidul IM, Brennan C, Wang Q, Mahmun MH. 2006. Convenient method of synthesizing 3-ethoxycarbonyl indoles. J Org Chem 71:4675–4677.

Sihna S, Watorek W, Karr S, Giles J, Bode W, Travis J. 1987. Primary structure of human neutrophil elastase. Proc Natl Acad Sci USA 84:2228–2232.

Sjö P. 2012. Neutrophil elastase inhibitors: recent advances in the development of mechanism-based and non-electrophilic inhibitors. Future Med Chem 4:651–660.

Spinks D, Armer RE, Miller DJ, Rankovic Z, Spinks G, Mestres J, Jaap DR. 2003. Preparation of 1-arylsulfonyl-3-sustituted indoles and indolines for the treatment of central nervous system disorders. PCT Int 2003068220.

Stockley R, De Soyza A, Gunawardena K, Perrett J, Forsman-Semb K, Entwistle N, Snell N. 2013. Phase II study of a neutrophil elastase inhibitor (AZD9668) in patients with bronchiectasis. Respir Med 107:524–533.

Sudhakara A, Jayadevappa H, Mahadevan KM, Hulikal V. 2009. Efficient synthesis of 2-ethoxycarbonyl indoles. Synth. Commun 39:2506–2515.

Tantak MP, Kumar A, Noel B, Shah K, Kumar D. 2013. Synthesis and biological evaluation of 2-arylamino-5-(3'-indoyl)−1,3,4-oxadiazoles as potent cytotoxic agents. Chem Med Chem 8: 1468–1474.

Tremblay GM, Janelle MF, Bourbonnais Y. 2003. Anti-inflammatory activity of neutrophil elastase inhibitors. Curr Opin Investig Drugs 4:556–565.

Veale CGL, Edkins AL, de la Mare JA, de Kock C, Smith PJ, Khanye SD. 2015. Facile synthesis and biological evaluation of assorted indolyl-3-amides and esters from a single, stable carbonyl nitrile intermediate. Tetrahedron Lett 56:1860–1864.

Vergely I, Laugaa P, Reboud-Ravaux M. 1996. Interaction of human leukocyte elastase with a *N*-aryl azetidinone suicide substrate: conformational analyses based on the mechanism of action of serine proteinases. J Mol Graphics 145:158–167.

Vogelmeier C, Aquino TO, O'Brien CD, Perrett J, Gunawardena KA. 2012. A randomised, placebo-controlled, dose-finding study of AZD9668, an oral inhibitor of neutrophil elastase, in patients with chronic obstructive pulmonary disease treated with tiotropium. COPD-J Chron Obstruct Pulmon Dis 9:111–120.

Von Nussbaum F, Li VMJ, Allerheiligen S, Anlauf S, Bärfacker L, Bechem M, Delbeck M, Fitzgerald MF, Gerisch M, Gielen-Haertwig H, et al. 2015. Freezing the bioactive conformation to boost potency: the identification of BAY 85-8501, a selective and potent inhibitor of human neutrophil elastase for pulmonary diseases. Chem Med Chem 10:1163–1173.

Voynow JA, Fisher BM, Zheng S. 2008. Proteases and cystic fibrosis. Int J Biochem Cell B 40:1238–1245.

Wang SF, Chuang CP. 1997. Manganese (III) acetate initiated oxidative free radical reaction between benzoylindoles and dimethyl malonate. Heterocycles 45:347–359.

Wang Z, Chen F, Zhai R, Zhang L, Su L, Thompson T, Christiani DC. 2009. Plasma neutrophil elastase and elafin imbalance is associated with acute respiratory distress syndrome (ARDS) development. Plos One 4:1–10.

Yuen Y, Choy PY, Chow WK, Wong WT, Kwong FY. 2013. Synthesis of 3-cyanoindole derivatives mediated by cooper (I) iodide using benzyl cyanide. J Org Chem 78:3374–3378.

Zhong J, Groutas WC. 2004. Recent developments in the design of mechanism-based and alternate substrate inhibitors of serine proteases. Curr Top Med Chem 4:1203–1216.